



**HAL**  
open science

## Performance of the JT-60SA cryogenic system under pulsed heat loads during acceptance tests

C Hoa, F Bonne, P Roussel, V Lamaison, S Girard, P Fejoz, R Goncalves, J Vallet, J Legrand, Y Fabre, et al.

### ► To cite this version:

C Hoa, F Bonne, P Roussel, V Lamaison, S Girard, et al.. Performance of the JT-60SA cryogenic system under pulsed heat loads during acceptance tests. Cryogenic Engineering Conference (CEC) 2017, Jul 2017, Madison (Wisconsin), United States. pp.012104, 10.1088/1757-899X/278/1/012104 . cea-04811349

**HAL Id: cea-04811349**

**<https://cea.hal.science/cea-04811349v1>**

Submitted on 29 Nov 2024

**HAL** is a multi-disciplinary open access archive for the deposit and dissemination of scientific research documents, whether they are published or not. The documents may come from teaching and research institutions in France or abroad, or from public or private research centers.

L'archive ouverte pluridisciplinaire **HAL**, est destinée au dépôt et à la diffusion de documents scientifiques de niveau recherche, publiés ou non, émanant des établissements d'enseignement et de recherche français ou étrangers, des laboratoires publics ou privés.



Distributed under a Creative Commons Attribution 4.0 International License

# Performance of the JT-60SA cryogenic system under pulsed heat loads during acceptance tests

C Hoa<sup>1</sup>, F Bonne<sup>1</sup>, P Roussel<sup>1</sup>, V Lamaison<sup>2</sup>, S Girard<sup>2</sup>, P Fejoz<sup>2</sup>, R Goncalves<sup>2</sup>, J C Vallet<sup>2</sup>, J Legrand<sup>3</sup>, Y Fabre<sup>3</sup>, V Pudys<sup>3</sup>, M Wanner<sup>4</sup>, A Cardella<sup>4</sup>, E Di Pietro<sup>4</sup>, K Kamiya<sup>5</sup>, K Natsume<sup>5</sup>, K Ohtsu<sup>5</sup>, M Oishi<sup>5</sup>, A Honda<sup>5</sup>, Y Kashiwa<sup>5</sup> and K Kizu<sup>5</sup>

<sup>1</sup> Univ. Grenoble Alpes, CEA INAC-SBT, Grenoble, 38000, France

<sup>2</sup> CEA, IRFM, Saint-Paul-lez-Durance, 13108, France

<sup>3</sup> Air Liquide Advanced Technologies, Sassenage, 38360, France

<sup>4</sup> Fusion for Energy, Garching, 85748, Germany

<sup>5</sup> QST, Naka Fusion Institute, Naka-shi, 311-0193, Japan

Email : Christine.hoa@cea.fr

**Abstract.** The JT-60SA cryogenic system a superconducting tokamak currently under assembly at Naka, Japan. After one year of commissioning, the acceptance tests were successfully completed in October 2016 in close collaboration with Air Liquide Advanced Technologies (AL-aT), the French atomic and alternative energies commission (CEA), Fusion for Energy (F4E) and the Quantum Radiological Science and Technology (QST). The cryogenic system has several cryogenic users at various temperatures: the superconducting magnets at 4.4 K, the current leads at 50 K, the thermal shields at 80 K and the divertor cryo-pumps at 3.7 K. The cryogenic system has an equivalent refrigeration power of about 9.5 kW at 4.5 K, with peak loads caused by the nuclear heating, the eddy currents in the structures and the AC losses in the magnets during cyclic plasma operation. The main results of the acceptance tests will be reported, with emphasis on the management of the challenging pulsed load operation using a liquid helium volume of 7 m<sup>3</sup> as a thermal damper.

## 1. Introduction

The cryogenic system of JT-60SA Super Advanced is a French voluntary contribution to the joint European - Japanese project [1], a superconducting tokamak presently under assembly at Naka, Japan. This fusion experiment is part of the Broader Approach agreement between Europe and Japan in order to support ITER and to investigate advanced plasma operation [2]. The tokamak will achieve deuterium plasmas with typical flat top durations of up to 100 seconds. The plasma will have a cyclic operation, inducing variable heat loads to be adsorbed by the cryogenic system. One of the challenging features of the refrigerator and the auxiliary cold boxes is to manage the pulse mode during plasma operation.

Dedicated tests were performed on a scaled down supercritical helium loop at CEA Grenoble [3] to assess the solution of a thermal damper to smooth the pulsed heat loads. ALAT designed and installed a 7 m<sup>3</sup> liquid helium bath to absorb the peak loads and not to disturb too drastically the refrigeration cold box and the warm compression station. The system is designed to absorb in average 6.5 kW at 4.5 K, and the thermal damper absorbs the peak loads up to 12 kW, with a limitation of temperature increase



of +0.4 K in the thermal damper. Without any heat load mitigation, the pressure and mass flow fluctuations would lead to an overloading of the warm compressors and a risk of turbine trip. Besides, the superconducting magnets shall be kept cold at [4.4, 4.8] K with mass flow variation below 20%. The pressure in the quasi-isochoric supercritical helium loops is expected to increase [3].

The installation and pre-commissioning activities have been described in [4]. The commissioning with the refrigeration and auxiliary cold boxes was completed in October 2016 and first reported in [5] and [6]. The present paper will focus on the acceptance tests defined in the acceptance test protocol. The different operating modes have been successfully tested. The performance of the cryogenic system under pulsed heat loads will be detailed and discussed.

## 2. Commissioning process

The cryogenic system is composed of a Warm Compression Station (WCS), a Refrigeration Cold Box (RCB) and an Auxiliary Cold Box (ACB) [7]. The simplified process flow diagram is shown in figure 1. The cryogenic system has been commissioned without connecting the circuits of the cryogenic users, using by-pass circuits equipped with electrical heaters simulating the thermal loads, and control valves for adjusting the pressure drops. There are five cooling loops:

- Loop 1 at 4.4 K: a supercritical helium cooling loop for the toroidal field (TF) coils and all cold structures driven by the cold circulator 1 at the nominal mass flow of 876 g/s, DP=130 kPa.
- Loop 2 at 4.4 K: a supercritical helium cooling loop for the Central Solenoid (CS) and Equilibrium field (EF) coils driven by the the cold circulator 2 at the nominal mass flow of 960 g/s, DP=80 kPa.
- Loop 3 at 3.7 K for the cryo-pumps, directly cooled by the main process flow with a mass flow of 270 g/s, DP=50 kPa.
- Loop 4 at 80 K for the thermal shields, with a nominal mass flow of 404 g/s, DP=150 kPa.
- Loop 5 at 50 K for the high temperature superconducting current leads, with a nominal mass flow of 25 g/s, DP=290 kPa. For the commissioning tests, a dedicated insulated line connects the 50 K supply line to an atmospheric heater, simulating the loads from the 50 K current leads.

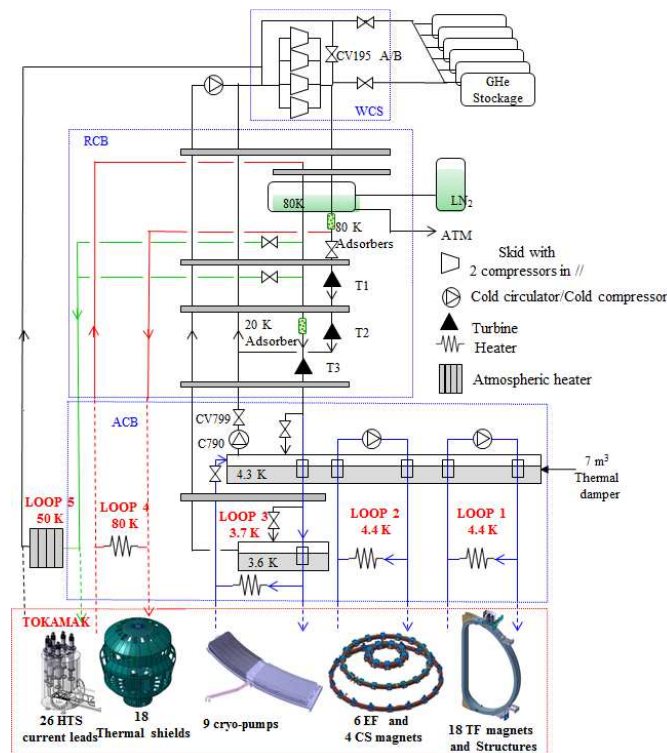


Figure 1. JT-60SA cryogenic system simplified flow process.

### 3. Definition of the operating modes

#### 3.1. Short stand-by mode (STS)

STS is foreseen during nights and weekends. The cold circulators are in reduced speed. The cold compressor can be stopped to save energy. The system has demonstrated a stable operation during a continuous operation of 36 hours in STS [6].

#### 3.2. Baking mode (BAK)

The system is in BAK mode every month, for one week in order to heat up the vacuum vessel to 473 K whereby the radiative loads at 80 K increase to 135 kW. The thermal shields can reach 140 K. During this mode, the coils are not energized and the nitrogen consumption is 3400 l/h. The system has demonstrated a stable operation during a continuous operation of 36 hours in BAK mode [5].

#### 3.3. Nominal mode (NOM)

NOM mode is composed of the plasma operation state (POS) and the dwell (DWE) period. During POS, the EF and CS are ramped up to start up the plasma, the plasma current is stabilized and then the EF and CS are ramped down. The large pulsed loads are generated during the POS and are first smoothed out through the helium circuits of the magnets and cryo-pumps, eventually evacuated through the cryo-distribution to the ACB thermal damper. Three different scenarios have been specified for the acceptance tests (table 1). For each scenario, the loads have been derived from a thermo-hydraulic model of the cooling circuits of the magnets [8]. The present paper will focus on the reference plasma scenario shown on figure 2. The loop 2 (EF and CS coils) has the most severe pulse load variation. In addition to these loads, the pumping powers of the cold circulator are deposited into the thermal buffer.

**Table1.** Scenarios during Normal operation mode (seconds).

	POS	DWE	TOTAL
Reference plasma scenario	170	1630	1800
Long plasma scenario	210	2790	3000
Long plasma scenario + disruption	210	3790	4000

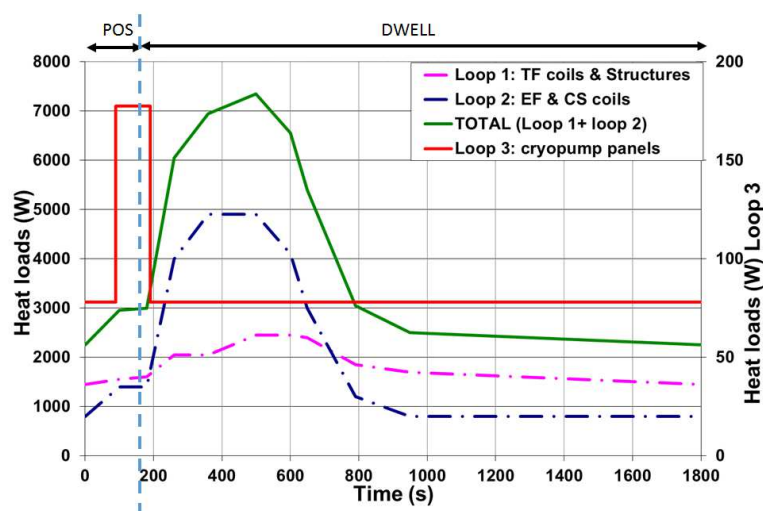


**Figure 2.** Reference scenario 60/1800s: heat load profiles (without the cold circulators pumping powers).

#### 4. Acceptance test protocol

For the commissioning tests, a detailed acceptance protocol was agreed, including functional tests and final acceptance tests to meet the performance requirements of the system [9].

##### 4.1. Functional tests

Prior to the acceptance test, the following functional tests were performed:

- Alarms, warnings and interlock signals tests
- Simulation of utility failure: loss of electrical power, instrument air and water cooling power
- Check of all the actuators, instrumentation and control system sequences
- Test and tuning of the turbines
- Characterizations of the cryo-machines: cold circulators and cold compressor at design operating point and at maximum speed (the surge and choke lines have been investigated for the cold circulators)
- Check of the temperature and mass flow measurements

##### 4.2. Uncertainties on measurements

The accuracy of the temperature measurement below 30 K, requiring high precision, could not meet the specification of 50 mK. This accuracy is difficult to meet with respect to all the uncertainties of the thermometric chain consisting of a calibrated Cernox sensor (1050-SD) installed in a thermometric block brazed on the stainless steel pipe or vessels and cabled to the temperature acquisition system CABTF™. Radiative inputs from the 300 K cryostat has been limited with multi-layer insulation (30 layers) and with a radiative shield around the thermometric block. The cabling wires to the temperature sensor were heat sunk to the helium process pipes. Temperature checks were performed, with respect to available reference temperatures from the saturated pressure of the liquid baths. Acceptance temperature criteria was fixed to  $T < 4.35$  K on the loops 1 and 2.

Several checks of the mass flow measurements at cryogenic temperatures have been performed with enthalpy balance calculation using the electrical heaters on each circuit. The mass flow were calculated using the ISO 5127 standards, depending on helium density, differential pressure measurement and discharge coefficient. Even though the Reynolds number range and diameter of the venturi were not applicable in the ISO 5127 standards, the discrepancies between the formula and the enthalpy balance calculation were ranging from 2% to 5% at nominal mass flows, close to the specification of 3% of uncertainty (table 2). This uncertainty increases drastically as the mass flow decreases, below the design condition of the venturi.

##### 4.3. Guaranteed values

The specified guaranteed values which were demonstrated by the final acceptance tests are listed in table 1 for the nominal mode of the five loops. The acceptance criteria were defined, taking into account the uncertainty of the measuring instruments (temperature, pressure and pressure drop). A few values do not strictly meet the acceptance criteria (bold values in table 2) but the deviations are small and only identified on a short time during the reference scenario. The loop 4 (thermal shields) inlet pressure is limited to 15.0 bara, due to the pressure drop between the WCS and the inlet of the ACB.

#### 5. Performance of the system in pulse operation mode

##### 5.1. Mitigations methods

The system can handle the variable loads with two complementary controls (figure 3):

- WCS capacity control: the warm compressor capacity is directly adapted to variable loads by controlling the LP at 1.05 bara. If the refrigeration power increases, the by-pass valve CV195A/B opening decreases. In a first step, the speed of the compressors equipped with the frequency drive is increased. In a second step, additional compressors can be switched on to take on the increase of loads. On the other hand when the loads decreases, the frequency drive

**Table 2.** Guaranteed and measured values during acceptance tests: reference plasma scenario.

	Uncertainty	Acceptance criteria	Measured values
<b>Loop 1</b>			
Temperature In (K)	> 0,055 K	$\leq 4.35$ (POS)/ $\leq 4.75$ (DWE)	$\leq 4.32$ (POS)/ $\leq 4.63$ (DWE)
Pressure In (bara)	+/- 0.1 bara	$\geq 5.4$	<b>5.32</b> -6.86
Pressure drop (kPa)	+/- 1 kPa	$\geq 131$ (POS)/ $\geq 51$ (DWE)	$\geq 131$ (POS)/ $\geq 52$ (DWE)
Mass flow (g/s)	+/- 3%	$\geq 876$ (POS)/ $\geq 444$ (DWE)	$\geq 876$ (POS)/ $\geq 444$ (DWE)
Heating power (W)	+/- 1%	figure 2	figure 3
<b>Loop 2</b>			
Temperature In (K)	> 0,055 K	$\leq 4.35$ (POS)/ $\leq 4.75$ (DWE)	$\leq 4.32$ (POS)/ $\leq 4.68$ (DWE)
Pressure In (bara)	+/- 0.1 bara	$\geq 4.9$	4.9-7.1
Pressure drop (kPa)	+/- 1 kPa	$\geq 81$	$\geq 82$
Mass flow (g/s)	+/- 3%	$\geq 960$	964-995
Heating power (W)	+/- 1%	figure 2	figure 3
<b>Loop 3</b>			
Temperature In (K)	> 0,055 K	$\leq 3.65$ (POS)/ $\leq 3.75$ (DWE)	$\leq 3.58$ (POS)/ $\leq 3.63$ (DWE)
Pressure In (bara)	+/- 0.1 bara	$\geq 4.75$	<b>4.66</b> -4.95
Pressure drop (kPa)	+/- 1 kPa	$\geq 51$	<b>50</b> -55
Mass flow (g/s)	+/- 3%	$\geq 270$	268-280
Heating power (W)	+/- 1%	figure 2	figure 2
<b>Loop 4</b>			
Temperature In (K)	+/- 0.66 K	$\leq 79.4$	79.9-80.4
Pressure In (bara)	+/- 0.1 bara	$\geq 15.1$	$\geq$ <b>14.9-15.0</b>
Pressure drop (kPa)	+/- 1 kPa	$\geq 151$	<b>136</b> -173
Mass flow (g/s)	+/- 3%	$\geq 404$	381-418
Heating power (W)	+/- 1%	42000	42700-43000
<b>Loop 5</b>			
Temperature In (K)	+/- 0.070 K	$\leq 51.93$	47.8-51.4
Pressure In (bara)	+/- 0.05bara	$\geq 4.05$	4.76-5.1
Pressure drop (kPa)	+/- 7 kPa	$\geq 297$	<b>291</b> -326
Mass flow (g/s)	+/- 3%	$\geq 25$	<b>24.8</b> -25.1

speeds decrease and eventually one or several compressors can be switched off. The mitigation method is well adapted for load variation on large time scale (1 hour) and will be used for adapting automatically the system in transient operation modes: from nominal to stand-by mode at night for example.

- Thermal buffer control: the 7 m<sup>3</sup> saturated liquid absorbs the peak loads by increasing the pressure control of the bath from 1.09 bara to 1.55 bara. A variable pressure control is performed with a split range function on the cold compressor speed and the opening valve of CV799 (figure 3). This mitigation method is suitable for load variation on a short time scale (1800 s, 3000 s and 4000 s pulse scenarios). It has the advantage to keep stable the refrigeration cold box and warm compression station, with limited mass flow and pressure variations. The mitigation is performed at the 4.5 K level in the auxiliary cold box.

### 5.2. Initial conditions before the acceptance test

Table 3 lists the control parameters for triggering the two complementary mitigation controls. The control parameters C0, C1 are related to the WCS capacity control, whereas C2, C3, C4 and C5 are related to the thermal damper controls, which have been tuned during commissioning to adapt the variation loads for the 1800 s, 3000 s and 4000 s scenarios.

In nominal operation, the cryogenic system is designed for an average 6.5 kW refrigeration power. The eight compressors were running at full capacity to keep a maximum margin on the warm compression station with a by-pass CV195 A/B > 15%. The Low Pressure (LP) is regulated at 1.05 bara. The high pressure (HP) control was set at the maximum pressure: 15.5 bara. The turbines have been tuned to maximize the refrigeration capacity. In the ACB, the loop 1 and loop 2 were set to

isochoric configuration, i.e. the supply and discharge valves were closed. Before the pulse starts, the helium bath is regulated to 1.09 bara/4.3 K with the cold compressor running at 177 Hz.

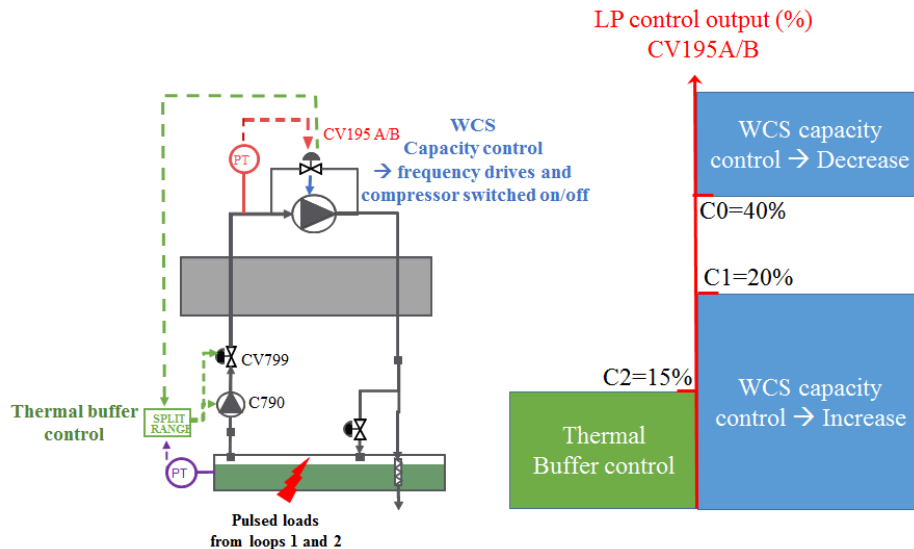


**Figure 3.** Thermal buffer and WCS capacity controls.

**Table 3.** Pulse mode control parameters during acceptance tests.

C0	LP output maximum limit to trigger WCS capacity decrease	40%
C1	LP output minimum limit to trigger WCS capacity increase	20%
C2	LP output minimum limit to trigger thermal Buffer operation	15%
C3	Maximum allowed thermal buffer pressure	1.55 bara
C4	Thermal buffer pressure set point	Ramp up rate 1 mbar/0,5 s
C5		Ramp down rate 1 mbar/2 s

### 5.3. Pulse test with thermal buffer control

The 60/1800 s pulsed load scenario was simulated by the heaters on loops 1 and 2 and transferred into the 4.3 K thermal damper (figure 2). The pulse loads increase during the first 500 s. In the meantime, the thermal buffer is pressurized, following the ramp up rate of 1 mbar every 0.5 s (C4), by reducing the speed of the cold compressor from 177 Hz to 35 Hz and then by throttling the control valve CV799 (figure 5). The thermal buffer reaches the maximum allowed pressure of 1.55 bara (C3) at  $t=600$  s (figure 5) and stabilizes for 30 s. Indeed during the dwell period, the specification of the inlet temperature of the loops is relaxed to a maximum value up to  $4.8 = 4.7 + 0.1$  K. Once the stability criteria is reached, the system releases the pulsed loads to the WCS ( $t= 600$  s to 1800 s). The bath pressure set point is decreased to 1.09 bara with a ramp down rate of 1 mbar every 2 s (C5). This parameter was adjusted with respect to the dwell time in order to recover the initial conditions before a new plasma shot starts. Hence, the control valve CV799 eventually opens to 100% and the cold circulator increases its speed to its nominal value of 177 Hz (figure 5).

### 5.4. Reference plasma scenario 60/1800 s

Figure 5 shows the heat load profiles applied on loop 1 and loop 2 during three consecutive reference plasma scenarios. This scenario is the most demanding in terms of refrigeration capacity, as the dwell time is the shortest to recover the initial conditions. The thermal buffer pressurizes from 1.09 bara up to 1.55 bara and the liquid level varies from 80% to 86% due mainly to the thermal expansion as the helium

mass in the thermal buffer does not vary much. The liquid level increase is slightly delayed (300 s) compared to the pressure signal. The time shift between the two signals can be explained by a small mass transfer and non homogeneity in temperature and pressure of this open volume connected to the LP and HP lines. At the end of each pulse, the pressures, the temperatures, the mass flows in all the circuits and the liquid levels in the 4,3 K and 3.6 K baths, recover their initial conditions.

Figure 6 shows the variations of the pressure and temperature, pressure drop and mass flow on the loop 1 and the loop 2. During dwell (170 s to 1600 s), the cold circulator of loop 1 is reduced from 276 Hz to 164 Hz. Consequently, the mass flow and the pressure drop are also reduced. The reduction of the pumping power enhances the capacity of the system to recover the liquid level. 200 s before the end of the cycle, the cold circulator 1 speed is increased back to 276 Hz so the loop can reach its initial conditions again before a new pulse starts. On the loop 2, the cold circulator remains at constant speed (240 Hz). The pulse loads induce a mass flow fluctuation of + 30 g/s, in accordance with a small increase of the pressure drop (81 to 85 kPa). As the two loops are isochoric, the pressure increases respectively from 5.3 bara to 6.9 bara for loop 1 and from 4.9 bara to 7.1 bar for loop 2.

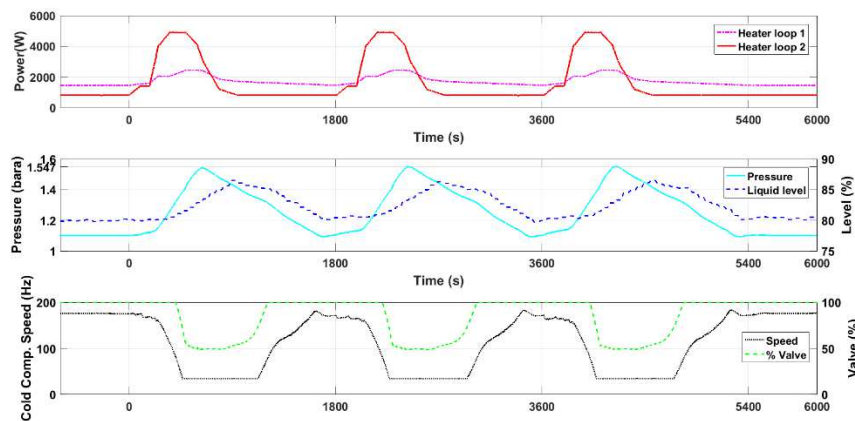


**Figure 4.** Three consecutive reference plasma pulses.

### 5.5. Discussion

A lot of pre-tests were necessary to tune the control parameters (table 3). The acceptance tests could be launched with automatic sequences and no manual operation by the operator was allowed during the tests in order to demonstrate the reliability and robustness of the controls. During commissioning tests, the three specified pulsed scenarios were tested and validated relying exclusively on the thermal buffer control, demonstrating the capability of the system to cope with high variable loads. The acceptance criteria could be met in terms of temperature, pressures, mass flow and dynamic heat loads. After three consecutive pulses, the initial liquid level of the thermal damper was recovered. The system has been sized with 5 % margin on the specified refrigeration loads. This margin could cover the additional heat losses on the system and the uncertainties on the mass flow and temperature measurements.

Additional tests, using the WCS capacity control could be tested to find mixed mitigation methods, with a relatively flexible warm compression station which could also take one part of the load variation. During tokamak operation, several different pulse load scenarios will occur. Some of the control parameters will have to be adjusted accordingly. Additional control tools could be useful to predict the thermal loads before they impact the thermal damper in the ACB. By analysing thermal hydraulic signals from the cryo-distribution and the magnets, the disturbances on the system could be better anticipated.

If the refrigeration capacity has been validated with the acceptance tests, challenging aspects related to control and reliability will have to be further addressed during future operation tests.



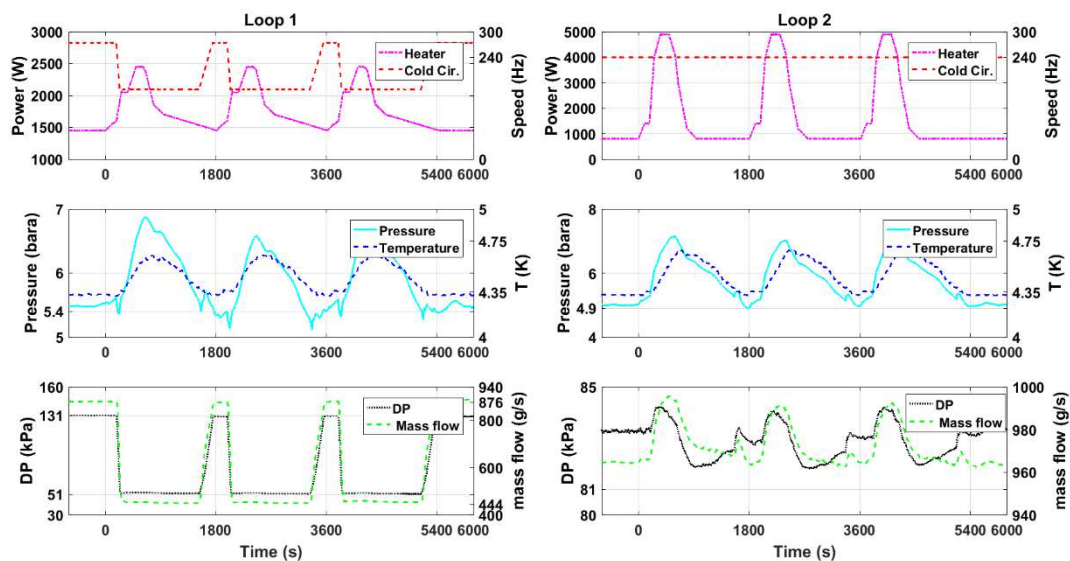


**Figure 5.** Reference scenario: loop 1 and loop 2 parameters.

## 6. Conclusion and perspectives

The JT-60SA cryogenic system has demonstrated the capacity to handle pulsed heat loads with automatic controls. The 7 m<sup>3</sup> thermal buffer could absorb the peak loads, preventing any large disturbance to the refrigeration cold box and the warm compression station. Dynamic modelling of the cryogenic system is under development and could be compared to the results of the commissioning tests. Model-based controllers could be investigated to address a large range of pulse load scenarios.

## 7. References

- [1] Vallet J-C et al. 2016 Towards the completion of the CEA Contributions to the Broader Approach Projects *Proc. 26th IAEA Fusion Energy Conference (Kyoto)*
- [2] Ishida S, Barabaschi P, Kamada Y and the JT-60SA Team 2010 Status and prospect of the JT-60SA project. *Fusion Engineering and Design*, 2070–79
- [3] Hoa C et al. 2015 Experimental and numerical investigations for the operation of large scale helium supercritical loops subjected to pulsed heat loads in tokamaks *Physic Procedia* **67** 54
- [4] Hoa C et al. 2016 Installation and pre-commissioning of the cryogenic system of JT-60SA tokamak *IOP Conference Series: Materials Science and Engineering*, **171** conference 1
- [5] Kamiya K et al. 2016 Commissioning of JT-60SA helium refrigerator. *Journal of Physics: Conference Series*
- [6] Hoa C et al. 2017 Commissioning results of JT-60SA cryogenic system, *Proc. IIR International Conference (Dresden)*
- [7] Lamaison V et al. 2010 Determination of heat loads at the interface of the JT-60SA cryogenic system *Proc. ICEC23-ICMC 2010 (Wroclaw)* 809
- [8] Michel F et al. 2012 Cryogenic Requirements for the JT-60SA Tokamak *Advances in Cryogenic Engineering* **57** 78-85
- [9] Lamaison V et al. 2014 Conceptual Design of the JT-60SA Cryogenic System *AIP Conf. Proc.* **1573**, 337